ELSEVIER

Chemical Engineering Journal 115 (2005) 73–83

Chemical Engineering Journal

www.elsevier.com/locate/cej

Determination of the kinetic parameters of fast exothermal reactions using a novel microreactor-based calorimeter

M.-A. Schneider, F. Stoessel *

Groupe de Sécurité des Procédés Chimiques, Institut des Sciences et Ingéniérie Chimique et Biochimique, Ecole Polytechnique Fédérale de Lausanne, Switzerland

Received 23 May 2005; received in revised form 14 September 2005; accepted 27 September 2005

Abstract

Making chemical processes safe requires a thorough knowledge of the kinetic and thermal parameters of the chemical reactions involved.

The aim of this work was to develop a calorimetric method particularly adapted to the study of fast exothermal reactions. The proposed system combines a microreactor with a commercially available microcalorimeter.

The microreactor was inserted into the cavity of the commercial calorimeter and the thermal efficiency of the system was optimized. The flow in the reaction channel of the microreactor was found to be purely laminar and the mixing time corresponded to the time for radial diffusion. Due to the small size of the channels, the mixing time was found to be adequate and not limiting for the characterization of fast reactions. First, a model reaction was studied in order to validate the results obtained with the microsystem and to avoid the risk of systematic errors. In a second stage, a previously unknown fast exothermal reaction was characterized. The heat flows measured during the reaction reached 160 000 W kg^{-1} but the conditions, however, remained completely isothermal. The global kinetics of this reaction as well as its activation energy were determined.

Keywords: Microreactor; Continuous flow; Microcalorimeter; Reaction kinetics; Exothermal reaction

1. Introduction

The assessment of the risks linked to the industrial practice of exothermal chemical reactions requires an extensive knowledge of their thermodynamic characteristics, not only under normal operation conditions, but also in the case of deviations. Since the risk is commonly assessed in terms of severity and probability of occurrence of a failure, it is essential to be able to predict under which conditions a reaction may enter a runaway course and what the consequences would be. The consequences of a runaway reaction are directly linked to the thermal potential of the reactions, i.e. to the energy released. The probability of triggering a runaway reaction is linked to the ability of maintaining its course under control. This means that the probability depends on the reaction dynamics. Thus the determination of the macro kinetics and of the enthalpy of both the main and potential secondary reaction(s) is required for the risk assessment. The safety analysis of a process is often performed by establishing a run-away scenario of the chemical system [1].

Kinetics can be determined by various methods. However, calorimetric methods are preferred for chemical process safety analyses, since they allow measuring directly the effect that should either be avoided or controlled. Many different calorimetric systems have been developed during the last decades [2,3]. However, fast and highly exothermal reactions are still difficult to characterize in classical systems. Indeed, measuring high heat release rates under isothermal conditions or at least under strict temperature control requires extremely high heat exchange rates. Moreover, such reactions should preferably be studied on a small scale, thus involving only small amounts of very reactive compounds. The use of small quantities is also an advantage when performing safety studies at an early stage of development, when large amounts of compounds are not available or are expensive. Finally, for fast reactions, rapid mixing as well as a precise control of the reaction start are mandatory.

The use of a microreactor-based calorimeter fulfills all of these requirements [4]:

- The high surface to volume ratio provides a highly efficient heat transfer,

* Corresponding author.

1385-8947/$ – see front matter © 2005 Elsevier B.V. All rights reserved.
doi:10.1016/j.cej.2005.09.019

- The small volume of the microchannel means that only small amounts of potentially dangerous chemicals are used,
- The small radius of the microchannel results in short time for radial diffusion and thus good mass transfer,
- The microreactor can be designed as a plug-flow reactor operating continuously at steady state. The reactants are mixed at the beginning of the reaction microchannel. This allows a good control of the reaction start as well as a measurement of the thermal effects as soon as the reactants mix, without any perturbation due to the mixing.

The microreactor can be associated with a commercially available calorimeter with a high thermal sensitivity.

In this work, a novel microreactor-based calorimeter is described and the performances of the system are first predicted using a finite element model. The degree of mixing achieved at the end of the reaction channel of the microreactor is then assessed, and the suitability of the system for the determination of reaction kinetics is verified using a model reaction. Finally, a fast exothermal reaction is investigated.

2. Experimental

2.1. Equipment

2.1.1. Layout of the system

The novel calorimetric system developed in this work uses the calorimetric measurement line of the Setline 120 microcalorimeter (Setaram, France).

Basic principle of the microcalorimeter [5,6]. In the standard measurement procedure recommended for this microcalorimeter, a crucible is introduced in the calorimetric cavity and placed on a microcalorimetric chip. The heat released or consumed by the chemical reaction induces a temperature difference between the thermocouples arranged in the center of the measurement membrane and a reference temperature outside the membrane.

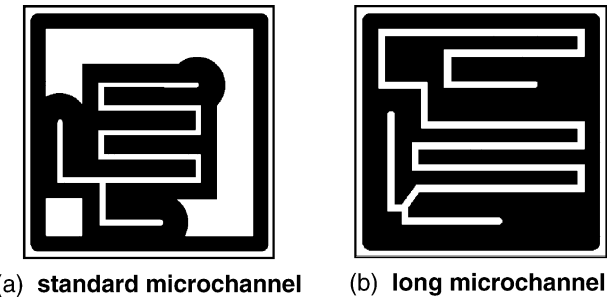

Fig. 2. Examples of reaction microchannels, width of 250 μm, depth of 100 μm and length of respectively 18.75 mm (a) and 44.00 mm (b).

This temperature difference is measured by a thermopile and the resulting signal is a voltage. This voltage (V) is then converted into a thermal signal (W) by calibration with Joule effect pulses applied by a heating resistance located on the calorimetric membrane.

In the present study, a microreactor was inserted in the calorimetric cavity replacing the crucible used in the standard procedure of the calorimeter. Fig. 1 represents a lateral section of the calorimetric cavity.

2.1.2. The reaction microchannel

The microchannel (b) was designed as a V-type or T-type mixer followed by a reaction tube of variable length.

The base of the microreactor was made of alumina (Al_2O_3) and the channel walls were built by silk-screen printing of a dielectric paste (ESL 4913, Electro-science Laboratories). The shape and the length of the reaction channel were adapted to the type of reaction. The slower the reaction rate, the longer the reaction channel.

Fig. 2 illustrates two examples of reaction microchannels.

The width of the microchannel was 250 μm and the depth 100 μm. The smaller reaction channel constructed had a length of 2.80 mm. The volume of the different microchannels constructed varied between 0.07 and 1.10 μl. The lower limit for the

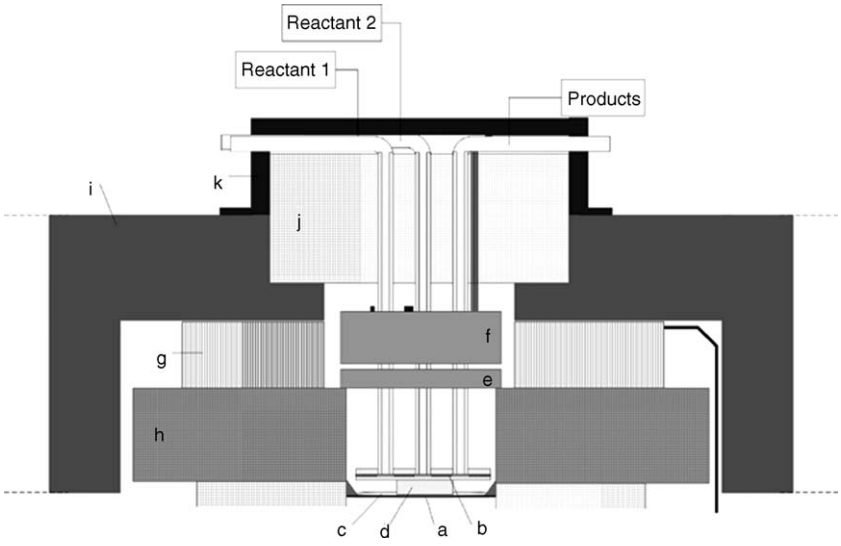

Fig. 1. Lateral section of the calorimetric cavity of the Setline 120 after insertion of the microreactor. (a) Microcalorimetric chip; (b) reaction channel; (c) heat carrier layer; (d) contact pin; (e) aluminum screen; (f) electrical preheating layer; (g) Peltier elements; (h) oven; (i) heat sink; (j) cap; (k) upper cap.

microchannel size is governed by the degree of mixing at the end of the channel, whereas the upper limit is given by the geometrical dimension of the microreactor base, i.e. of the calorimetric membrane.

2.1.3. Thermal efficiency of the system

The optimization of the thermal efficiency of the calorimeter was detailed in a previous publication [7] and is summarized and completed in this section.

As the thermocouples of the calorimeter are only arranged in the center of the calorimetric membrane (a square of 4 mm by 4 mm in the membrane of 8 mm by 8 mm (a)), a contact pin (d) made of alumina was glued below the reaction channel of the microreactor to direct the heat flow released in the reaction channel towards the sensor and to avoid heat losses in the non-sensitive part of the membrane. In addition, a heat carrier (c) (Polyethylene-glycol 300, Fluka, Switzerland) was put in between the contact pin and the microcalorimetric membrane in order to eliminate the air layer between these two elements and to improve the heat transfer. An aluminum screen (e) was glued to the inlet and outlet tubes, mimicking the screen present in the original configuration of the calorimeter. This screen ensured a reproducible positioning of the microreactor in relation to the microcalorimetric membrane. In addition, it formed a thermal bridge above the oven that allowed the preheating of the incoming fluids. An electrical preheating layer (f) was also added in order to provide a sufficient preheating of the incoming fluid especially at high temperatures and high flow rates and for reactions with weak heat flows. This avoided the tedious calibration of the sensible heat. This preheating layer was made of two different layers: an alumina layer on which two resistances were deposited by silk-screen printing (one to heat the plate and the other to measure the temperature reached) and a 4 mm thick aluminum block glue-bonded to the alumina plate. The addition of the thick aluminum block distributed the heat generated by the heating resistance vertically and thus increased the contact surface with the tubes.

An upper cap was added on top of the existing cap to maintain the position of the outgoing tubes and avoid any movement of the microreactor during the replacement of the reagent-containing syringes. It also improved the contact between the aluminum screen and the oven, and between the contact pin and the membrane, by applying a small mechanical force on the microreactor.

Fig. 3 is a picture of the current version of the microreactor.

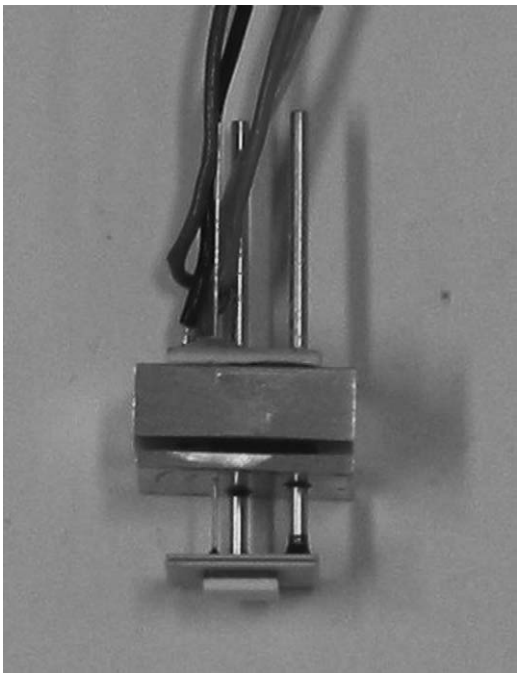

Fig. 3. Picture of the microreactor inserted in the calorimetric cavity of the Setline 120.

2.2. Methods

2.2.1. Assessment of the mixing in the microchannel by laser-induced fluorescence measurements

A modified version of the microreactor was developed to allow fluorescence measurements in the microchannel. The alumina base was replaced by a glass layer (see Fig. 4) and the channels were built using a vitreous paste (DP QQ600, Dupont).

The fluorescent dye SNARF-5F (Molecular Probes, Netherland) was introduced in the reaction channel and excitation was achieved by a YAG laser at 543 nm. The dye chosen showed a pH dependent absorbance. The emission of this dye was maximal at 630 nm at a pH of 9 and decreased almost to 0 at a pH of 5.

One milligram of the dye was dissolved in 100 ml of distilled water. NaOH was added to set the pH of the resulting solution at 9 ($c_{NaOH} = 1.0 \times 10^{-3}$ mol l^{-1}). The solution was prepared using a 1 M NaOH solution (Aldrich). A sulphuric acid solution at pH 3 ($c_{H_2SO_4} = 1.1 \times 10^{-3}$mol l^{-1})was also prepared (using H_2SO_4 puriss. p.a. 95–97%, Fluka). The alkaline solution was introduced in a first syringe; a second syringe contained the acidic solution. At the end of the channel, the pH of the mixed solution was 4. At this pH, there was no fluorescence emission of the dye. Proton diffusion was measured by following the decrease of the dye fluorescence.

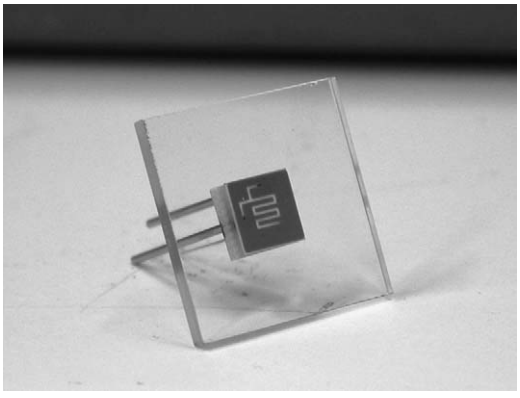

Fig. 4. Picture of the microreactor constructed for the assessment of the degree of mixing in the reaction channel by laser-induced fluorescence measurements.

2.2.2. Thermal calibration of the system

The heat released in the channel can be distributed in different ways in the calorimetric cavity. However only the heat distributed in the sensitive part of the microcalorimetric membrane is measured; the heat distributed in other directions leads to heat losses. Each time a novel microreactor is inserted in the calorimetric cavity, a calibration has to be performed to correlate the heat flow released in the microchannel by the chemical reaction $\dot{q}_{rx}$with the heat flow effectively measured $\dot{q}_{meas}$(heat distributed in the sensitive part of the microcalorimetric membrane). This ratio is called the thermal efficiency and is used as a correction factor, F, in all subsequent experiments:

$$F = \frac{\dot{q}_{\text{measured}}}{\dot{q}_{rx}} \quad (1)$$

This ratio allows the quantification of heat losses. What determines the thermal efficiency is the quality of the thermal contact between the reactor and the sensors of the calorimetric membrane.

The thermal calibration of the system was performed using the neutralization reaction of H_2SO_4 by NaOH.

Standard calibration. The standard calibration was performed at heat flows corresponding to the one expected for the model reaction i.e. heat flows lower than 1 mW. The flow rate in the reaction channel was set at 4 μl min^{-1} (2 μl min^{-1} for each feed stream) and the following initial concentration of NaOH and H_2SO_4 were used: 0, 0.1, 0.2, 0.3 and 0.4 mol l^{-1}. The temperature was 40 °C.

Calibration at high heat flows. This calibration was performed to check the linearity of the experimental points at higher concentrations and higher flow rates. The neutralization of H_2SO_4 0.6 mol l^{-1} with NaOH 0.6 mol l^{-1} was performed at 40 °C with flow rates of the feed streams varying from 10 to 25 μl min^{-1}.

2.2.3. Validation of the system with the kinetic study of a model reaction—the saponification of ethyl acetate with NaOH

The saponification of ethyl acetate in alkaline solution was selected as model reaction for the validation of the novel calorimetric system (see reaction (I)). This reaction is fairly fast, exothermal and well-described in literature [8–11]. The reaction kinetics is of second-order.

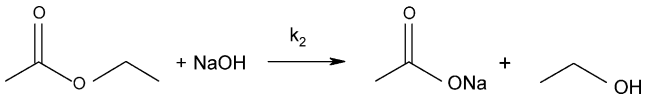

(I)

Ethyl acetate (ethyl acetate anhydrous 99.8%, Aldrich) was diluted in water to obtain the various concentrations used. As ethyl acetate slowly hydrolyzes at room temperature, fresh solutions had to be used for each experiment. The alkaline solutions were obtained by dilution in water of a standard 1 mol l^{-1} NaOH solution. The longer microchannel design (see Fig. 2) was used for these experiments.

Determination of the reaction enthalpy. This was achieved by choosing temperature and concentration conditions ensuring complete conversion at the end of the channel.

The concentration of ethyl acetate was set at 0.1 mol l^{-1}, the concentration of sodium hydroxide was 1 mol l^{-1} and the temperature was 40 °C. The flow rates of the feed streams were varied from 0 to 5 μl mol^{-1}. The calculation of the reaction enthalpy was done following the technique described in Section 3.1.

Determination of the kinetic parameters. The reaction of ethyl acetate 0.8 mol l^{-1} with NaOH 1 mol l^{-1} was performed at five different temperatures ranging from 30 to 70 °C. The residence time in the reaction channel was changed by varying the flow rate of the entering fluids. The flow rates of the feed streams were varied from 0 to 6 μl min^{-1}.

2.3. Reaction generating high heat flows

The suitability of the system for the characterization of reactions involving high heat flows was assessed by studying the reaction of an unsaturated ether (designated ether A) in a methanolic solution of H_2SO_4 2.5%.

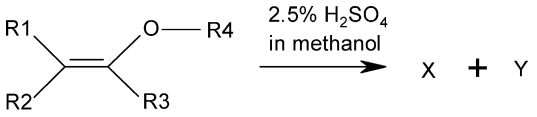

Ether A (II)

Ether A was used without dilution in a solvent. The standard microchannel design (see Fig. 2) was used for these experiments.

Determination of the reaction enthalpy. The temperature was set at 40 °C and the flow rates of the feed streams ranged from 0 to 13 μl min^{-1}.

Determination of the kinetic parameters. The temperature was varied from 40 to −5 °C. The flow rates ranged between 0 and 13 μl min^{-1}.

In the temperature scanning mode experiments, the flow rate was maintained constant and the temperature was varied at the rate of 0.6 °C min^{-1}. In the five experiments performed, the flow rate ranged between 2 and 11 μl min^{-1}.

3. Theory

The determination of reaction kinetics in a continuous system is considerably different from the one used in a discontinuous system. At steady state, the conversion achieved at the end of the reaction channel depends on the residence time in the channel i.e. on the flow rate of the feed streams. The signal measured corresponds to the average signal along the reaction channel.

3.1. Determination of the enthalpy of reaction

For the determination of reaction kinetics, the first step is to experimentally measure the enthalpy of reaction. The heat flow measured can be written as follows:

$$\dot{q}_{rx} = \dot{V} c_0 (-\Delta H_R) X \quad (2)$$

Combining Eq. (1) with Eq. (2) gives:

$$\frac{\dot{q}_{\text{measured}}}{F} = \dot{V}c_0(-\Delta H_R)X = \dot{N}X(-\Delta H_R) \quad (3)$$

From Eq. (3) one can deduce that for $X = 1$, the slope of the plot of the corrected heat flow versus the molar flow rate ($\dot{q}_{\text{measured}}/F = f(\dot{V}c_0) = f(\dot{N})$)gives the enthalpy of reaction. The enthalpy of reaction can thus be determined either by maintaining the concentration constant and varying the flow rate or inversely by maintaining the flow rate constant and varying the concentration.

3.2. Determination of the conversion achieved at the end of the channel

When a reaction is not completed at the end of the channel, the conversion rate can be calculated using Eq. (3) and knowing the enthalpy of reaction:

$$X = \frac{\dot{q}_{\text{measured}}}{F\dot{V}(-\Delta H_R)c_0} \quad (4)$$

The variation of the flow rate allows calculating the conversion at the end of the channel at various residence times in the microchannel.

3.3. Determination of the kinetic constant k

The calculation of the kinetic constant k depends obviously on the order of reaction. In the following paragraph the equations needed for the calculation of k are derived for reactions kinetics of first- and second-order. These derivations are explained in more details by Levenspiel [12].

3.3.1. For a first-order reaction

The rate equation can be written as follows:

$$\frac{dc_A}{dt} = k_{1st}c_A \quad (5)$$

Eq. (5) can be rewritten in terms of conversion and integrated giving:

$$k_{1st} = -\frac{1}{t}\ln(1 - X) \quad (6)$$

Eq. (6) allows the calculation of k_{1st}.

3.3.2. For a second-order reaction

The rate equation of a second-order reaction involving two species A and B can be written:

$$\frac{dc_A}{dt} = k_{2nd}c_Ac_B \quad (7)$$

Supposing that the amounts of A and B are not always added in stoichiometric proportions,

$$c_{A0}\frac{dX}{dt} = k_{2nd}(c_{A0} - c_{A0}X)(c_{B0} - c_{A0}X) \quad (8)$$

Letting $M = c_{A0}/c_{B0}$ and after simplification, Eq. (8) becomes:

$$\frac{dX}{dt} = k_{2nd}c_{A0}(1 - X)(M - X) \quad (9)$$

which after integration and simplification gives,

$$k_{2nd} = -\frac{1}{(c_{B0} - c_{A0})t}\ln\left(\frac{1 - X}{1 - MX}\right) \quad (10)$$

The energy of activation and the frequency factor are then simply obtained by linearization of the Arrhenius equation. The slope of the plot of $\ln k = f(1/T)$ allows the determination of the activation energy E_a and the ordinate at the origin provides the frequency factor k_0.

4. Calculations

4.1. Simulation of the theoretical limit of thermal explosion

The construction of this novel calorimetric system was governed by the necessity of characterizing fast and exothermal reactions. Preliminary predictions of the system performance were therefore computed by a simplified model using finite elements. The range of heat flows that would allow to work in isothermal condition was first predicted.

The limit for thermal explosion and the limit for maintaining isothermal conditions were compared with a calorimetric system classically used in safety laboratories, the differential scanning calorimeter DSC.

This model allows the calculation of the temperature profile in the reactor as a function of the heat release rate.

4.1.1. Hypothesis and parameters of the model

The major hypothesis for this simulation is that the heat is transferred by conduction only, i.e. no contribution of convection to heat transfer is taken into account. This hypothesis is valid for the microchannel, but is more debatable in the case of the DSC crucible, which has a larger volume. In order to rend the problem one-dimensional, the crucible was treated as a thermally equivalent sphere and the microchannel as an equivalent infinite cylinder. Using the dimension of a standard DSC crucible, the radius of the equivalent sphere calculated is 1.6 mm. For the microchannel, a rectangular shape of 250 μm width and 100 μm depth is taken into consideration; the corresponding hydraulic radius is then 72 μm.

The heat transfer coefficient is estimated, from experimental measurements, as 500 $\text{W m}^{-2}\text{ K}^{-1}$ for the DSC crucible and as 10 000 $\text{W m}^{-2}\text{ K}^{-1}$ for the microchannel. The other parameters of the model were defined as follows: $\lambda = 0.1\text{ W m}^{-1}\text{ K}^{-1}$, $\rho = 1000\text{ kg m}^{-3}$, $C_p = 1800\text{ J kg}^{-1}\text{ K}^{-1}$, $E_a = 100\,000\text{ J mol}^{-1}$.

The geometries were divided into 100 concentric layers and a thermal balance was calculated for each element using finite elements.

4.1.2. Comparison of the microsystem with a DSC calorimeter

For both systems, the heat flow released in the reactor was varied and the corresponding increase of the temperature profile

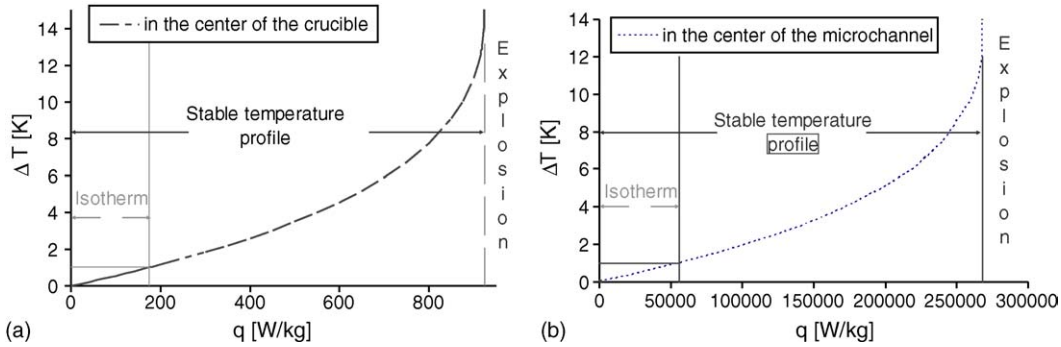

Fig. 5. Comparison of the limit of thermal explosion in a DSC crucible (a) and in the microchannel (b).

was calculated. Isothermal conditions were defined as a deviation of the temperature at the center of the sample of less than 1 °C. A thermal explosion occurs when no stable temperature profile can be established.

The conclusions of Fig. 5 are summarized in Table 1.

In the microchannel, strictly isothermal conditions were predicted to be maintained even for heat flow 300 times higher than in a DSC crucible (Table 1).

4.1.3. Comparison of the microsystem with an adiabatic calorimeter

Adiabatic calorimeters are typically used for the study of the decomposition of highly exothermal compounds. One of the best performing equipment for such studies is the APTAC from Setaram, which can follow temperature increases up to 400 °C min^{-1}.

In an adiabatic calorimeter, a heat flow of 56 000 W kg^{-1} (limit for isothermal conditions in the microchannel calculated in the preceding subsection) corresponds to a temperature increase of 1866 °C min^{-1} (see Eq. (11)).

$$\frac{dT}{dt} = \frac{\dot{q}}{C_p} = \frac{56\,000}{1800} = 31.1\,(^{\circ}\mathrm{C\,s^{-1}}) \Rightarrow 1866\,(^{\circ}\mathrm{C\,min^{-1}}) \tag{11}$$

This heat flow is too high to be measured even in an adiabatic calorimeter.

4.2. Simulation of the kinetics determination in the microchannel using computational fluid dynamics

CFD simulations were performed with the mathematical program FEMLAB (Comsol, Sweden) to check the suitability of the microchannel for the determination of reaction kinetics. The Navier–Stokes equation for incompressible fluid defined the velocity profile, whereas the solute concentration profile was calculated with the convection–diffusion model.

Table 1
Summary of the calculated limits for isothermal conditions and of thermal explosion for both systems

Instrument	DSC crucible (W kg^{-1})	Microchannel (W kg^{-1})
Limit for isothermal conditions	175	56000
Limit of thermal explosion	923	268000

The reaction of ethyl acetate 0.8 mol l^{-1} with NaOH 1.0 mol l^{-1} was computed.

The predicted variation of the ethyl acetate concentration along the channel is represented in Fig. 6a for a linear velocity of the feed streams of 9.33×10^{-4} m s^{-1} (corresponding to 1.4 μl min^{-1}) and a temperature of 70 °C.

A cross-section plot of the concentration of ethyl acetate at the end of the reaction channel is represented in Fig. 6b. The concentration of ethyl acetate calculated is compared to the initial concentration in the channel. This allows calculating the conversion achieved at the end of the channel.

By varying the inlet velocities, the conversion can be calculated for various residence times. One can check that the conversions predicted by simulation are similar to those calculated from the expression of the reaction rate, using the same kinetic parameters, but without taking the geometry into account.

As seen in Fig. 7, both calculations correlate well. Thus there is no influence of the flow established in the microchannel on the evaluation of the reaction kinetics. According to these predictions, the mixing time does not affect the results.

5. Results

5.1. Assessment of the degree of mixing

The efficiency of a microreactor highly depends on the degree of mixing achieved in the reaction channel. This is especially true for fast reactions where mixing can be the rate limiting step. Thus the knowledge of the flow regimen and of the mixing time are important issues for the determination of reaction kinetics. The most common way for characterizing a flow is the calculation of the Reynolds number.

Reynolds number (*Eq.* (*12*)). This parameter allows distinguishing a laminar regimen from a turbulent regimen:

$$Re = \frac{\rho u d_h}{\mu} \tag{12}$$

The flow rates used in the microreactor ranged between 1 and 40 μl min^{-1}. Eq. (12) was used to estimate the Reynolds number for each different flow rate. The corresponding Reynolds numbers varied between 0.1 and 4.2. These values correspond to a laminar regimen.

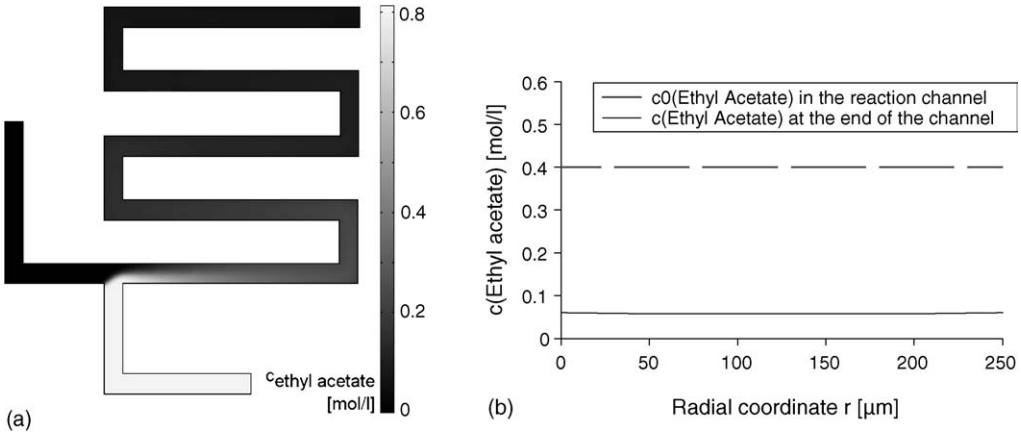

Fig. 6. Simulation of the reaction of ethyl acetate 0.8 mol l^{-1} with NaOH 1.0 mol l^{-1} with linear velocities at the inlets of 9.33×10^{-4} m s^{-1}, $T = 70\,^{\circ}$C. (a) Concentration of ethyl acetate along the channel; (b) cross plot section at the end of the channel.

This was checked experimentally using laser-induced fluorescence measurements.

Experimental assessment using LIF measurements. Fig. 8 shows a picture of the mixing taken in a standard microchannel (see Fig. 2) with a flow rate of the feed stream of 2 µl min^{-1}. The white fluid represents the dye in the alkaline solution and the black fluid the acidic solution.

At the inlet of the microchannel, the inlet streams were clearly separated. The flow is clearly laminar. A small area of diffusion can be observed between the two layers. At the end of the channel, mixing is completed. The time required for complete diffusion is found to be close to the time of radial diffusion of the protons. This corresponds to 0.5 s in the microchannels.

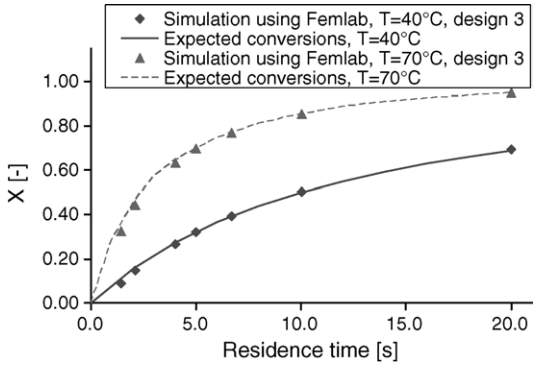

Fig. 7. Simulations of the conversion at the end of the channel at $T = 40\,^{\circ}$C and $T = 70\,^{\circ}$C. Comparison with the one predicted without taking the geometry into account.

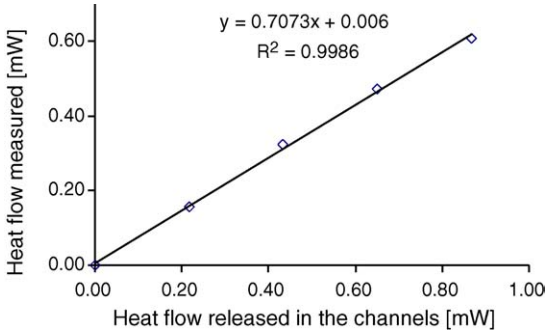

Fig. 9. Calibration of the novel calorimetric system, flow rate in the microchannel of 4 µl min^{-1}, concentration of H_2SO_4 and NaOH ranging from 0 to 0.4 mol l^{-1}.

5.2. Calibration of the calorimetric system

5.2.1. Standard calibration

The regression of the experimental signal versus the calculated heat in the reaction channel was perfectly linear. The correction factor F was 0.71 (see Fig. 9).

Thus more than 70% of the heat released in the reaction channel was measured. The rest was mainly lost in the non-sensitive part of the microcalorimetric membrane.

5.2.2. Calibration at high heat flows

As shown in Fig. 10, linearity was maintained up to the highest heat flows tested corresponding to 12.00 mW, i.e. 25 000 W kg^{-1}.

Fig. 8. Visualization of the mixing in the reaction channel by LIF measurement: (a) microchannel inlet; (b) microchannel outlet. The white fluid represents the fluorescent dye; the black fluid the acidic solution. Flow rate of the feed streams of 2 µl min^{-1}.

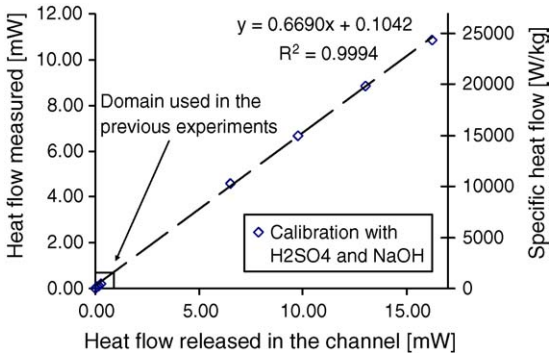

Fig. 10. Calibration reaction: neutralization of H_2SO_4 0.6 mol l^{-1} by NaOH 0.6 mol l^{-1} at 40 °C at flow rates varying from 10 to 25 μl min^{-1}.

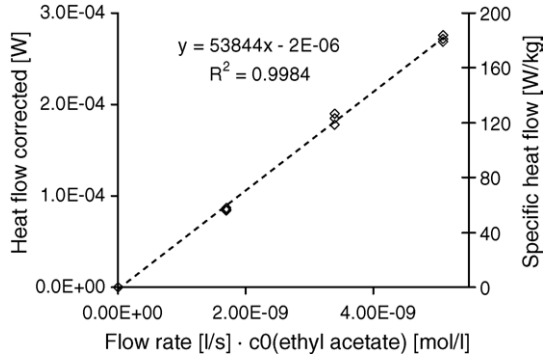

Fig. 11. Saponification of ethyl acetate 0.1 mol l^{-1} by NaOH 1 mol l^{-1} at 40 °C: determination of the reaction enthalpy.

5.3. Validation of the system using a model reaction

Reaction enthalpy. The linearity of the experimental points with the molar flow rate confirmed that the conversion was complete at the end of the channel and the reaction enthalpy could therefore be estimated.

The reaction enthalpy given by the slope of Fig. 11, i.e. 53.8 kJ mol^{-1}.

Kinetic parameters. The concentrations were then changed to slow down the reaction and study the kinetics (Fig. 12).

The experimental conversions were then used to calculate the corresponding kinetic constant k_{2nd} for each point using Eq.

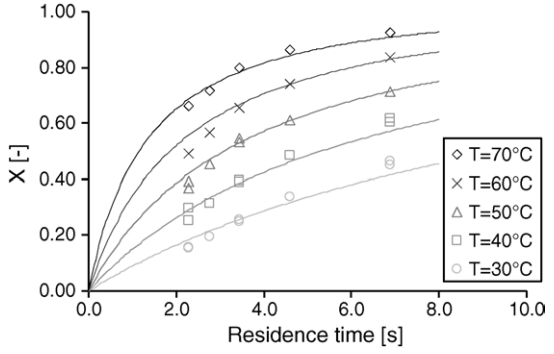

Fig. 12. Saponification of ethyl acetate 0.8 mol l^{-1} by NaOH 1 mol l^{-1} at five temperatures: determination of the kinetic parameters.

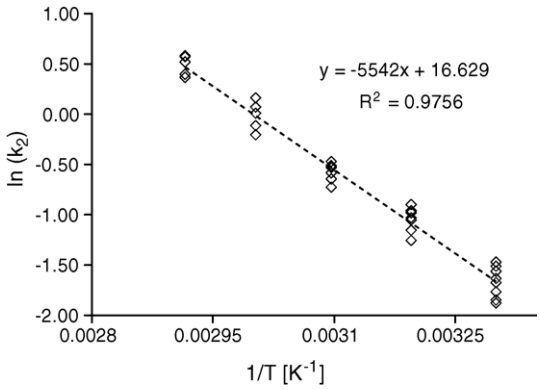

Fig. 13. Arrhenius plot drawn from the data of Fig. 12. Determination of the activation energy.

(10) developed in Section 3.3. The activation energy obtained from the Arrhenius plot of Fig. 13 was 46.1 kJ mol^{-1}. The kinetic parameter k_{2nd} can be extrapolated at 25 °C and is 0.140 l mol^{-1} s^{-1}.

The range of specific heat flows measured in this experiment varied from 50 to 170 W kg^{-1}.

5.4. Kinetic determination of an unknown fast exothermal reaction

The study of the reaction of unsaturated ether A with 2.5% H_2SO_4 in methanol (see (I)) was then investigated.

Determination of the reaction enthalpy. The reaction enthalpy was first determined experimentally and corresponded to 41.4 kJ mol^{-1} (Fig. 14). The thermal signal measured was strictly linear with the molar flow up to the highest specific heat flow tested corresponding to 160 000 W kg^{-1}. Higher heat flows could not be tested since heat saturation of the calorimeter was reached.

This value of reaction enthalpy was confirmed by control measurements in a Calvet calorimeter.

Determination of the kinetic parameters. The order of reaction was first determined by varying the concentrations (results not shown).

Fig. 15 shows the conversion rates achieved at the various flow rates and temperatures tested.

The activation energy of the reaction was 35.7 kJ mol^{-1} and the frequency factor 5.8×10^6 s^{-1}.

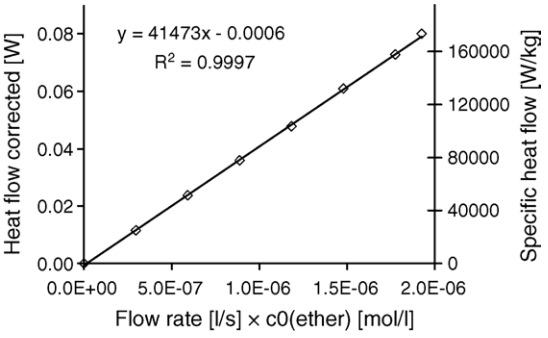

Fig. 14. Reaction of the unsaturated ether with a methanolic solution of H_2SO_4 2.5% at 40 °C—determination of the reaction enthalpy.

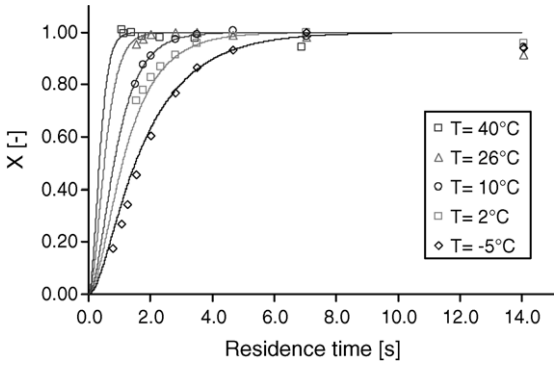

Fig. 15. Reaction of the unsaturated ether with a methanolic solution of H_2SO_4 2.5% at five different temperatures—determination of the kinetic parameters.

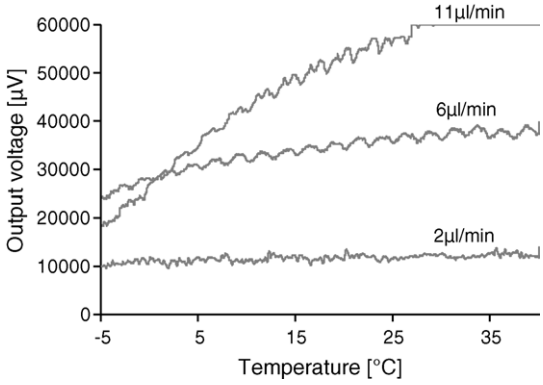

Fig. 16. Raw data of the calorimeter obtained in temperature-scanning mode with the reaction of the unsaturated ether with a methanolic solution of H_2SO_4 2.5%.

Temperature-scanning mode. The kinetic parameters obtained in isothermal mode were compared with those obtained in temperature-scanning mode. In Fig. 16, for visibility reasons, only three of the five experiments performed are shown.

For each experiment i.e. each flow rate, conversion values were calculated for five selected temperatures corresponding to the five isotherms performed. In Fig. 17, these values were compared with the conversion values predicted by the fit of the isothermal experiments (see Fig. 15).

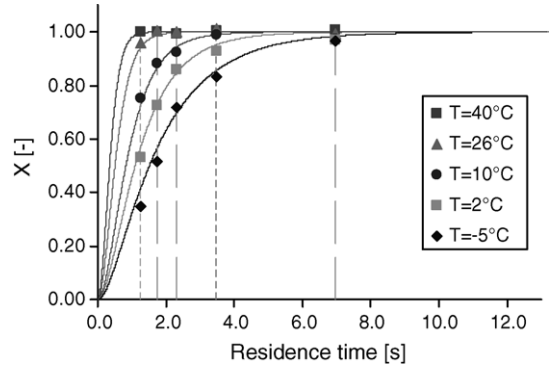

Fig. 17. Comparison of the results in temperature-scanning mode with the results in isothermal mode. Points: conversion calculated for the temperature-scanning mode, curve: fit of the isothermal mode.

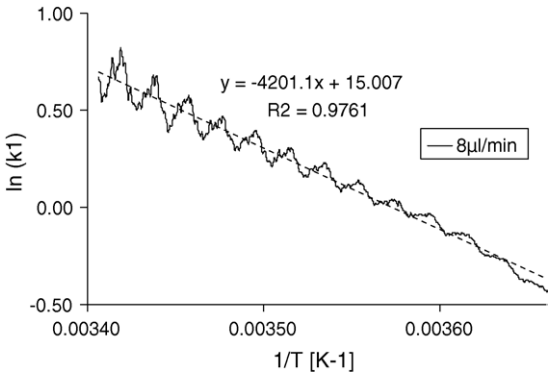

Fig. 18. Example of determination of the activation energy of the reaction using a single scan—flow rate is 8 µl min^{-1}.

From a single scan, the activation energy can be obtained (Fig. 18). The activation energy determined with this technique was 34.9 kJ mol^{-1}. This value is close to the activation energy determined with the isothermal mode technique i.e. 35.7 kJ mol^{-1}.

The deviation of the value obtained from one scan to the other was however sometimes close to 15%. Several scans are therefore needed to obtain a precise value of the activation energy.

6. Discussion

6.1. Mixing

In a previous publication [7], the results obtained with the Dushman reaction (iodate-iodide system) were presented and the Bodenstein number was calculated. A laminar regimen with a residence time distribution corresponding to an ideal plug flow was predicted.

In the present paper, the Reynolds number were calculated and ranged between 0.1 and 4.2. According to the literatures [13,14], in tubular channels, the flow is laminar for Reynolds numbers below 2100 and turbulent above this value. However some recent publications have cast some doubt on the application of this theory in the case of microchannels. The relatively high roughness of microchannels might reduce the critical Reynolds number for the transition from laminar to turbulent flow. Peng et al. [15] detected transitions to turbulence flow at Reynolds numbers between 200 and 700, with the transition value depending on the hydraulic diameter. This was however contradicted by Pfund [16]. The latter took into account the pressure drop within the channel itself to exclude entrance and exit losses and considered also the surface roughness of the channel for its calculation. Transitions to turbulence were observed with flow visualization. For smaller width channels, the transition occurred at a Reynolds number of 1700.

In any case, the Reynolds numbers achieved in our microchannel are considerably lower than the critical Reynolds number for transition to turbulent flow. Therefore laminar flow can be assumed in the entire application range of our microsystem. This has an important consequence since it means that mixing occurs only by diffusion and not by convection as in the case of turbulent flow.

This prediction was confirmed by the results obtained by laser-induced fluorescence. The flow observed using this method was shown to be purely laminar and the mixing time corresponded to the time for radial diffusion. The flow in the microchannel occurred almost as predicted. The flow was not stuck in the angles. The two inlet streams were parallel and did not enter in the reaction channel in small blocks. No unexpected phenomenon was observed. The CFD simulation confirmed moreover that the predicted mixing time would not interfere with the kinetics determination.

The time of mixing in this system remains a current limitation of this system. A mixing time close to 0.5 s for proton diffusion can be limiting when working with fast reaction. This limitation is emphasized when solely organic molecules are involved as the molecular diffusion constant will be lower. This mixing time could however be improved by optimizing the geometry of the microchannel using for example multi-lamination at the inlets [17].

6.2. Validation of the system with a model reaction

The enthalpy of the model reaction determined experimentally was $-53.8\,\mathrm{kJ\,mol^{-1}}$ in good agreement with the value reported in the literature $-54.7\,\mathrm{kJ\,mol^{-1}}$ [9,10]. The error is less than 2%. The activation energy of $46.1\,\mathrm{kJ\,mol^{-1}}$ obtained experimentally was close to the value of $47.3\,\mathrm{kJ\,mol^{-1}}$ reported by Kirby [8]. Concerning the kinetic constant, Papoff and Zambonin [9] observed that this value depends on the concentration of NaOH and measured a k_{2nd} at 25 °C of $0.141\,\mathrm{l\,mol^{-1}\,s^{-1}}$ with NaOH $1\,\mathrm{mol\,l^{-1}}$ in excellent agreement with the value obtained in our experiments ($0.140\,\mathrm{l\,mol^{-1}\,s^{-1}}$).

These results validate the suitability of the system for the determination of reaction kinetics.

6.3. Isothermal conditions

In the finite element modeling presented in Section 4 the calculated limits (limit for isothermal conditions and limit of explosion) are probably slightly too strict in the case of the crucible as the convection is not taken into account but this provides anyway an interesting approximation. The low value of $175\,\mathrm{W\,kg^{-1}}$ obtained for the crucible is thus due to the hypothesis of pure conduction but also to the strict definition of isothermal conditions.

In the case of the novel calorimetric system, isothermal conditions are predicted to be maintained up to a specific heat flow of $56\,000\,\mathrm{W\,kg^{-1}}$.

Actually our experiments showed that this prediction was even an underestimation. The difference observed with the prediction is probably due to the strict definition of isothermal condition used in the model. It could also be due to an underevaluation of the heat transfer coefficient.

In fact, during the determination of the reaction enthalpy of the unsaturated ether A with methanolic acidic solution (in Fig. 14), the linearity of the experimental points was maintained up to specific heat flows of $160\,000\,\mathrm{W\,kg^{-1}}$. This proved that there was no heat accumulation in the outlet fluid i.e. that isothermal conditions were maintained. The thermal and kinetic study of the fast exothermal reaction could easily and quickly be performed in the novel system.

7. Conclusion

The microreactor-based system developed in our laboratory opens new possibilities in the isothermal characterization of fast and highly exothermal reactions. This technique allows to obtain precise results very quickly. An unknown reaction involving an unsaturated ether that could not be characterized in classical calorimeter was studied and its kinetics and thermal parameters could be found. Isothermal conditions were obtained until specific heat flows of $160\,000\,\mathrm{W\,kg^{-1}}$ which is more than one order of magnitude higher than classical calorimeters. Moreover it can be run in a scanning mode to obtain a first rapid approximation of the activation energy of a reaction. The limitation due to the mixing time in the channel could be improved in further microreactors by optimizing the geometry of the microchannel.

Acknowledgments

Hoffmann-la-Roche AG Division Pharma and DSM Nutritional Product are acknowledged for their financial support, F. Mascarello and J. Schildknecht for very fruitful discussions. The microreactors were constructed by the laboratory of microtechnical production, Institute of Production and Robotics, EPFL who are acknowledged for their collaboration in this project. The LIF measurements were made in collaboration with Dantec Dynamics (Erlangen, Germany).

References

[1] F. Stoessel, Design thermally safe semi-batch reactors, Chem. Eng. Prog. 91 (9) (1995) 46–53.
[2] R.J. Willson, Calorimetry, in: P.J. Haines (Ed.), Principles of Thermal Analysis and Calorimetry, RSC, 2002, pp. 129–165.
[3] G. Höhne, Thermal analysis and calorimetry, in: J. Wiley (Ed.), Ullman's Encyclopedia of Industrial Chemistry, Wiley–VCH, 2000.
[4] W. Ehrfeld, V. Hessel, H. Löwe, Microreactors, New Technology for Modern Chemistry, Wiley–VCH, 2000.
[5] A.W. Van Herwaarden, P.M. Sarro, Thermal sensors based on the seebeck effect, Sens. Actuators 10 (3–4) (1986) 321–346.
[6] J. Lerchner, A. Wolf, G. Wolf, Recent developments in integrated circuit calorimetry, J. Therm. Anal. Calorimetry 57 (1) (1999) 241–251.
[7] M.-A. Schneider, et al., A microreactor-based system for the study of fast exothermic reactions in liquid phase: characterization of the system, Chem. Eng. J. 101 (2004) 241–250.
[8] A.J. Kirby, in: C.H. Bamford, C.F.H. Tipper (Eds.), Comprehensive Chemical Kinetics, Elsevier, Amsterdam, 1972.
[9] P. Papoff, P.G. Zambonin, Applicability of the quasi-adiabatic enthalpimetric method for the study of chemical kinetics, Talanta 14 (1967) 581–590.
[10] A. Roux, et al., Enthalpies of reaction and reaction rates by flow microcalorimetry: ester hydrolysis in basic medium, J. Sol. Chem. 9 (1980) 59–73.
[11] R.E. Johnson, R.L. Biltonen, Determination of reaction rate parameters by flow calorimetry, J. Am. Chem. Soc. 97 (9) (1975) 2349–2355.

[12] O. Levenspiel, Interpretation of batch reactor data, in: O. Levenspiel (Ed.), Chemical Reaction Engineering, 1999, pp. 38–65.
[13] R.W. Flumerfelt, Transport phenomena, in: J. Wiley (Ed.), Ullman's Encyclopedia of Industrial Chemistry, Wiley–VCH, 2000.
[14] R. Felder, R. Rousseau, Elementary Principles of Chemical Processes, Wiley, 1986.
[15] X.F. Peng, G.P. Peterson, B.X. Wang, Heat transfer characteristics of water flowing through microchannels, Exp. Heat Transf. 7 (1994) 265.
[16] D. Pfund, et al., Pressure drop measurements in a microchannel, AIChE J. 46 (8) (2000) 1496–1507.
[17] T.M. Floyd, et al., in: W. Ehrfeld (Ed.), Novel Liquid Phase Microreactors for Safe Production of Hazardous Speciality Chemicals. Microreaction technology/IMRET 3, 2000, pp. 171–180.